



Available online at <http://scik.org>

Commun. Math. Biol. Neurosci. 2020, 2020:64

<https://doi.org/10.28919/cmbn/4906>

ISSN: 2052-2541

NON-NEWTONIAN HEAT AND MASS TRANSFER ON MHD BLOOD FLOW THROUGH A STENOSED ARTERY IN THE PRESENCE OF BODY EXERCISE AND CHEMICAL REACTION

ANNORD MWAPINGA^{1,*}, EUNICE MUREITHI², JAMES MAKUNGU², VERDIANA MASANJA¹

¹Department of Applied Mathematics and Computational Sciences, The Nelson Mandela African Institution of Science and Technology, P.O.Box 447, Arusha, Tanzania

²Department of Mathematics, University of Dar es salaam, P.O. Box 35091 Dar es Salaam, Tanzania

Copyright © 2020 the author(s). This is an open access article distributed under the Creative Commons Attribution License, which permits unrestricted use, distribution, and reproduction in any medium, provided the original work is properly cited.

Abstract. A mathematical model of non-Newtonian blood flow, heat and mass transfer through a stenosed artery is studied. The non-Newtonian model is chosen to suit the Herschel-Bulkley fluid characteristics, taking into account the presence of body acceleration, magnetic fields and chemical reaction. The study assumed that, the flow is unsteady, laminar, two-dimensional and axisymmetric. The governing flow equations of motion were solved numerically using explicit finite difference schemes. The study found that velocity profile diminishes with increase in Hartman number and increases with body acceleration. The temperature profile is raised by the increase of body acceleration and the Eckert number, while it diminishes with the increase of the Peclet number. It was found also that the concentration profile increases with the increase of the Soret number and decreases with the increase of the chemical reaction. It was further observed that the shear stress deviates more when $n > 1$ than when $n < 1$. Shear stress for power law fluid when $n > 1$ exhibited higher magnitude value than Newtonian, Bingham and Herschel-Bulkley fluids.

Keywords: herschel-bulkley fluid; non-newtonian; magnetic field; chemical reaction.

2010 AMS Subject Classification: 76A05.

*Corresponding author

E-mail address: mwapingaa@nm-aist.ac.tz

Received August 3, 2020

1. INTRODUCTION

The cardiovascular system involves blood, the heart and the blood vessel. Blood is important because it is a transporting agent in the human body. It is very unfortunate that the human blood vessels such as arteries and capillaries may contain plaques which disturb the normal flow of blood and hence leading to cardiovascular diseases such as heart attack and stroke. The abnormal flow of blood has drawn attention to many researchers due to its implications in medicine and fluid mechanics.

Blood is categorically classified as a non-Newtonian fluid, thus studies which involve modelling blood flow should not disregard the non-Newtonian character of blood. In day to day activities, human body is exposed to situation which disturb the normal flow of blood. This include (among others), physical exercises, travelling using vehicles and applying magnetic therapy to a patient.

A number of investigators have carried out theoretical studies on blood flow. Misra et al [15] modeled blood flow in arteries subject to the vibrating environment. In their study, the fluid (blood) was treated as a couple stress fluid. However, their study did not take into consideration the presence of stenoses despite the fact that human arteries are often subjected to fat or solid deposits that lead to constricted arterial wall.

A recent study of non-Newtonian blood flow in a stenosed artery that was conducted by Liu and Liu [14] involved the flow of blood in a tapered artery and took into consideration heat and mass transfer. The study established that as the maximum depth of the stenosis increases, the blood's axial velocity increases. Another study on blood flow in a stenosed artery was done by Jamil et al [12] that took into consideration the effects periodic body acceleration and nanoparticles. It was proved that velocity decreases as yield stress increases and the velocity could be controlled by nanoparticles. Numerical solution of blood flow and mass transport in an elastic tube with multiple stenoses was also investigated by Alsemiry et al [3], where blood was treated a Newtonian fluid. The result of their study was that the double stenoses and pulsatile inlet conditions increase the number of recirculation regions and effect higher mass transfer rate at the throat. Changdar and De [6] conducted a similar study like Alsemiry et al [3] but considered the presence of body acceleration. As it was expected, the result revealed that the

presence of body acceleration enhances the axial velocity.

Computational modelling of arterial blood flow for non - Newtonian fluid was investigated (in *in vitro*) by Sharma and Yadav [18], Jamalabadi et al [1], Dixit et al [7] and Prasad and Yasa [16]. These studies did not include the aspect of vibration or body acceleration and the heat transfer in the body which is very important to take into consideration. On the other hand, Bunonyo et al [5], Eldesoky [8] and Sinha et al [19] studied MHD blood flow along the arterial wall. However, all these studies, the aspect of body acceleration and mass transfer were not investigated. As expected, all these studies showed among other things, that magnetic fields affect the blood's velocity.

Arteries as living tissues, require supply of metabolites, including oxygen, and removal of waste products, Akbar et al [2]. Zaman et al [23], pointed out that, it is generally accepted that the rheological behavior of blood is assumed as Newtonian for values of shear rate greater than $100s^{-1}$ and a such situation occurs in larger arteries. But in smaller arteries the blood does not obey the Newtonian postulate and therefore cannot be modeled as a Newtonian fluid. Several more scholars conclude that it is very crucial that blood is model as a non – Newtonian fluid. These include Rodkiewicz et al [17], Tu and Deveille [21], and Gijsen et al [9].

There are several theoretical studies which have attempted to model blood flow in arteries by considering blood to obey the Herschel-Bulkley fluid characteristics. These include studies by Srivastava[20] and Kumar and Gupta et al [13]. All these studies assumed unidirectional blood flow. The Herschel-Bulkley fluid is of general type and can be reduced to Newtonian, Bingham plastic and Power-law fluid models, by selecting appropriate flow parameters, Biswas and Laskar [4]. According to Vajravelu et al,[22], the Herschel-Bulkley constitutive equation contains one more parameter than the Casson equation does, and thus more information about the blood properties can be obtained when the Herschel-Bulkley equation is used than when the Casson one is used.

Based on the reviewed literature, the unsteady, MHD flow of blood through a stenosed artery in the presence of body acceleration, chemical reaction, with mass and heat transfer taking place, and treating blood as Herschel-Bulkley fluid, has not been considered. Such flows have manifested themselves in several situations like magnetic therapy in sports and in MRI testing. The

current study therefore intends to fill that gap where, computational analysis of unsteady non – Newtonian MHD blood flow involving heat and mass transfer in the presence of body acceleration and chemical reaction is investigated.

2. FORMULATION OF THE PROBLEM

In the current study we consider that the flow is unsteady, laminar, two-dimensional, pulsatile, incompressible, axisymmetric in the sense that there is no variation of the velocity with the angle θ in the cylindrical polar coordinate system (r, θ, z) , with the z -axis coinciding with the axis of symmetry of the flow. In that regard therefore, $u_\theta = 0$ and $\frac{\partial \mathbf{u}}{\partial \theta} = 0$. The blood is considered to be a non - Newtonian fluid satisfying the Herschel-Bulkley model. Furthermore, body acceleration $(F(t))$, and the strength of magnetic field (B_0) act in the axial direction of the artery. Every cell in the body can produce heat which needs to be spread around the body, and this is done by the blood, which heats some organs and cools others by conduction and other processes. Thus, the study takes into account for the chemical reaction such as exothermic reaction K for mass transfer.

We define the geometry of stenosis as shown in equation (2.1)

$$(2.1) \quad R(z) = \begin{cases} r_0 - \delta \left(1 + \cos \frac{\pi z}{2z_0} \right) & -2z_0 \leq z \leq 2z_0 \\ r_0 & \text{otherwise} \end{cases}$$

Under the mentioned assumptions, the governing blood flow equations, continuity, momentum, energy and concentration equations in the cylindrical polar coordinate system are as written in equations (2.2) to (2.6).

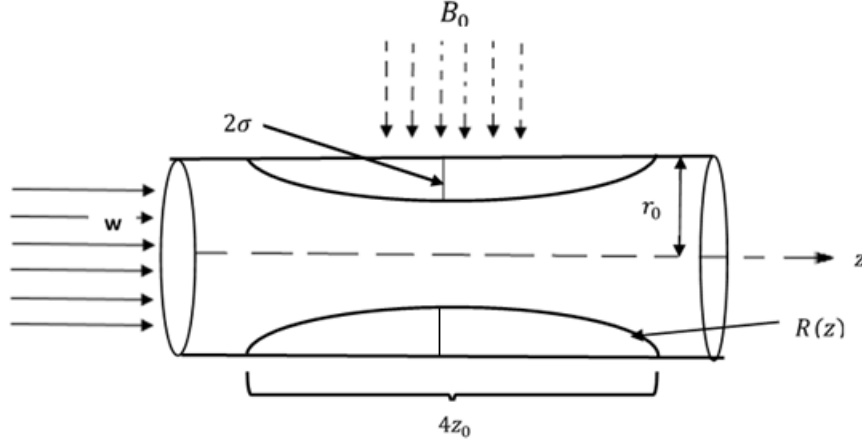


FIGURE 1. Schematic flow diagram

$$(2.2) \quad \frac{\partial u}{\partial r} + \frac{u}{r} + \frac{\partial w}{\partial z} = 0$$

$$(2.3) \quad \rho \left(\frac{\partial u}{\partial t} + u \frac{\partial u}{\partial r} + w \frac{\partial u}{\partial z} \right) = -\frac{\partial P}{\partial r} + \frac{1}{r} \frac{\partial (r\tau_{rr})}{\partial r} + \frac{\partial (\tau_{rz})}{\partial z}$$

$$(2.4) \quad \rho \left(\frac{\partial w}{\partial t} + u \frac{\partial w}{\partial r} + w \frac{\partial w}{\partial z} \right) = -\frac{\partial P}{\partial z} + \frac{1}{r} \frac{\partial (r\tau_{rz})}{\partial r} + \frac{\partial (\tau_{zz})}{\partial z} + F(t) - \sigma B_0^2 w$$

(2.5)

$$\rho c_p \left(\frac{\partial T}{\partial t} + u \frac{\partial T}{\partial r} + w \frac{\partial T}{\partial z} \right) = k \left(\frac{\partial^2 T}{\partial r^2} + \frac{1}{r} \frac{\partial T}{\partial r} + \frac{\partial^2 T}{\partial z^2} \right) + \tau_{rr} \frac{\partial u}{\partial r} + \tau_{rz} \frac{\partial w}{\partial r} + \tau_{rz} \frac{\partial u}{\partial z} + \tau_{zz} \frac{\partial w}{\partial z}$$

$$\left(\frac{\partial C}{\partial t} + u \frac{\partial C}{\partial r} + w \frac{\partial C}{\partial z} \right) = D_f \left(\frac{\partial^2 C}{\partial r^2} + \frac{1}{r} \frac{\partial C}{\partial r} + \frac{\partial^2 C}{\partial z^2} \right) + \frac{D_f K_T}{T_0} \left(\frac{\partial^2 T}{\partial r^2} + \frac{1}{r} \frac{\partial T}{\partial r} + \frac{\partial^2 T}{\partial z^2} \right)$$

$$(2.6) \quad -\beta(C - C_0)$$

In the above equations, u , w , T and C are respectively radial velocity, axial velocity, temperature and concentration of the fluid. c_p, k, K_T, D_f , and β are, respectively the specific heat capacity, thermal conductivity, the thermal-diffusion ratio, diffusion coefficient, and chemical reaction parameter. Furthermore, τ_{rr} , and τ_{zz} represent the normal stress components. τ_{rz} is the

shear stress component. The current study considers that blood obeys the Herschel-Bulkley constitutive model. The stress tensor components are as given in equation (2.7)

$$(2.7) \quad \begin{aligned} \tau_{ij} &= \left(K\dot{\gamma}^{n-1} + \frac{\tau_0}{\dot{\gamma}} \right) \dot{\gamma}_{ij} \quad \text{for } \tau \geq \tau_0 \\ \dot{\gamma} &= 0 \quad \text{for } \tau < \tau_0 \end{aligned}$$

where, K is the consistency index, n is the flow behavior index and τ_0 is the yield stress at zero shear rate. From equation (2.7) there are special cases that can arise as we can be able to see different types of behaviors of fluids. This is as shown in table 1.

Type of fluid model	K	n	τ_0
Herschel-Bulkley	>0	$0 < n < \infty$	>0
Newtonian	>0	1	0
Power law for $n < 1$ (shear-thinning)	>0	$0 < n < 1$	0
Bingham	>0	1	>0
Power law for $n > 1$ (shear-thickening)	>0	$1 < n < \infty$	0

TABLE 1. Different types of behaviors of fluids

In equation (2.7), $\dot{\gamma}$ is the second invariant of the rate of strain which is as given in equation (2.8).

$$(2.8) \quad \dot{\gamma} = \sqrt{2 \left[\left(\frac{\partial u}{\partial r} \right)^2 + \left(\frac{u}{r} \right)^2 + \left(\frac{\partial w}{\partial z} \right)^2 \right] + \left(\frac{\partial u}{\partial z} + \frac{\partial w}{\partial r} \right)^2}$$

Again, from equation (2.7) we can write the stresses

$$(2.9) \quad \tau_{rr} = 2 \left(K\dot{\gamma}^{n-1} + \tau_0\dot{\gamma}^{-1} \right) \left(\frac{\partial u}{\partial r} \right)$$

$$(2.10) \quad \tau_{zz} = 2 \left(K\dot{\gamma}^{n-1} + \tau_0\dot{\gamma}^{-1} \right) \left(\frac{\partial w}{\partial z} \right)$$

$$(2.11) \quad \tau_{rz} = 2 \left(K\dot{\gamma}^{n-1} + \tau_0\dot{\gamma}^{-1} \right) \left(\frac{\partial u}{\partial z} + \frac{\partial w}{\partial r} \right)$$

The pulsatile pressure gradient which is responsible for driving the blood's flow in the axial direction is given as $-\frac{\partial P}{\partial z} = A_0 + A_1 \cos(\omega t)$, $t > 0$ where, we define A_0 and A_1 as the steady component of pressure gradient and amplitude of its pulsatile component respectively. $\omega = 2\pi f_p$, f_p being the pulse frequency. We further define the body acceleration which acts in our system as $F(t) = \rho a_0 \cos(\omega_b t + \psi)$ where, ρa_0 is the amplitude of body acceleration, ψ is the phase angle and $\omega_b = 2\pi f_b$, with f_b the body acceleration frequency.

2.1. Boundary and initial conditions. In this study we assume that initially as shown in equation (2.12) that;

$$(2.12) \quad w(r, z, 0) = w_0, \quad T(r, z, 0) = T_0, \quad C(r, z, 0) = C_0,$$

The boundary conditions for the developed model are as shown in equations (2.13) to (2.16).

$$(2.13) \quad w(r, z, t) = 0, \quad u(r, z, t) = 0 \quad \text{on} \quad r = R(z)$$

$$(2.14) \quad \frac{\partial w(r, z, t)}{\partial r} = 0, \quad u(r, z, t) = 0 \quad \text{on} \quad r = 0$$

$$(2.15) \quad \frac{\partial T(r, z, t)}{\partial r} = 0, \quad \text{on} \quad r = 0 \quad \text{and} \quad T(r, z, t) = T_w \quad \text{on} \quad r = R(z)$$

$$(2.16) \quad \frac{\partial C(r, z, t)}{\partial r} = 0, \quad \text{on} \quad r = 0 \quad \text{and} \quad C(r, z, t) = C_w \quad \text{on} \quad r = R(z)$$

Where, T_w , C_w stands for arterial wall temperature and concentration on the arterial wall, respectively.

3. NON - DIMENSIONALISATION OF THE MODEL VARIABLES

We now introduce the non-dimensional variables. We use w_c as the average fluid's velocity which is therefore our characteristic velocity. We define r_0 as the radius of normal artery. Our dimensionless variables are shown in equations (3.1) to (3.3).

$$(3.1) \quad \eta = \frac{r}{r_0}, w^* = \frac{w}{w_c}, u^* = \frac{u}{w_c}, \quad t^* = \frac{tw_c}{r_0}, z^* = \frac{z}{r_0}, P^* = \frac{P}{\rho w_c^2}, \quad \tau_{ij}^* = \frac{\tau_{ij}}{\rho w_c^2},$$

$$(3.2) \quad A_0^* = \frac{A_0 r_0}{\rho w_c^2}, A_1^* = \frac{A_1 r_0}{\rho w_c^2}, \omega^* = \frac{r_0 \omega}{w_c}, \omega_b^* = \frac{r_0 \omega_b}{w_c}, \quad a_0^* = \frac{r_0 a_0}{w_c^2}, \quad R^*(z^*) = \frac{R(z)}{r_0}$$

$$(3.3) \quad T^* = \frac{T - T_0}{T_w - T_0}, \quad C^* = \frac{C - C_0}{C_w - C_0}, \quad \beta^* = \frac{\beta r_0^2}{\nu}, \quad e = \frac{\delta}{r_0}.$$

We now substitute equations (3.1) to (3.3) into equations (2.2) to (2.16) so that after dropping all the asterisks, we get equations (3.4) to (3.16).

$$(3.4) \quad \frac{\partial u}{\partial \eta} + \frac{u}{\eta} + \frac{\partial w}{\partial z} = 0$$

$$(3.5) \quad \frac{\partial u}{\partial t} + u \frac{\partial u}{\partial \eta} + w \frac{\partial u}{\partial z} = \frac{\partial P}{\partial \eta} + \left(\frac{\partial \tau_{rr}}{\partial \eta} + \frac{1}{\eta} \tau_{rr} + \frac{\partial \tau_{rz}}{\partial z} \right)$$

$$\frac{\partial w}{\partial t} + u \frac{\partial w}{\partial \eta} + w \frac{\partial w}{\partial z} = (A_0 + A_1 \cos(\omega t)) + \left(\frac{\partial \tau_{rz}}{\partial \eta} + \frac{1}{\eta} \tau_{rz} + \frac{\partial \tau_{zz}}{\partial z} \right)$$

$$(3.6) \quad + a_0 \cos(\omega_b t + \psi) - \frac{H_a^2}{ReG} w$$

$$\frac{\partial T}{\partial t} + u \frac{\partial T}{\partial \eta} + w \frac{\partial T}{\partial z} = \frac{1}{Pe} \left(\frac{\partial^2 T}{\partial \eta^2} + \frac{\partial T}{\eta \partial \eta} + \frac{\partial^2 T}{\partial z^2} \right)$$

$$(3.7) \quad + E_c \left[\tau_{rr} \frac{\partial u}{\partial \eta} + \tau_{rz} \frac{\partial w}{\partial \eta} + \tau_{rz} \frac{\partial u}{\partial z} + \tau_{zz} \frac{\partial w}{\partial z} \right]$$

$$\frac{\partial C}{\partial t} + u \frac{\partial C}{\partial \eta} + w \frac{\partial C}{\partial z} = \frac{1}{Pe} \left(\frac{\partial^2 C}{\partial \eta^2} + \frac{1}{\eta} \frac{\partial C}{\partial \eta} + \frac{\partial^2 C}{\partial z^2} \right)$$

$$(3.8) \quad + S_r \left(\frac{\partial^2 T}{\partial \eta^2} + \frac{1}{\eta} \frac{\partial T}{\partial \eta} + \frac{\partial^2 T}{\partial z^2} \right) - \frac{\beta C}{Re}$$

Where, $ReG = \frac{r_0^n \rho}{K w_c^{n-2}}$, $Ha = B_0 \sqrt{\frac{\sigma r_0^{n+1}}{K w_c^{n-1}}}$, $Pe = \frac{\rho w_c r_0 c_p}{k}$, $E_c = \frac{w_c^2}{c_p (T_w - T_0)}$ and $S_r = \frac{D_f K_T (T_w - T_0)}{\nu T_m (C_w - C_0)}$ are the, generalized Reynold, Hartman, Peclet, Eckert, and Soret numbers respectively.

$$(3.9) \quad \tau_{ij} = \left(\frac{1}{ReG} \dot{\gamma}^{n-1} + \tau_0 \dot{\gamma}^{-1} \right) \dot{\gamma}_{ij}$$

$$\dot{\gamma} = 0 \quad \text{for} \quad \tau < \tau_0$$

with second invariant of the rate of strain given in equation (3.10)

$$(3.10) \quad \dot{\gamma} = \sqrt{2 \left[\left(\frac{\partial u}{\partial \eta} \right)^2 + \left(\frac{u}{\eta} \right)^2 + \left(\frac{\partial w}{\partial z} \right)^2 \right] + \left(\frac{\partial u}{\partial z} + \frac{\partial w}{\partial \eta} \right)^2}$$

and

$$(3.11) \quad \tau_{rr} = 2 (R_e G \dot{\gamma}^{n-1} + \tau_0 \dot{\gamma}^{-1}) \left(\frac{\partial u}{\partial \eta} \right)$$

$$(3.12) \quad \tau_{zz} = 2 (R_e G \dot{\gamma}^{n-1} + \tau_0 \dot{\gamma}^{-1}) \left(\frac{\partial w}{\partial z} \right)$$

$$(3.13) \quad \tau_{rz} = 2 (R_e G \dot{\gamma}^{n-1} + \tau_0 \dot{\gamma}^{-1}) \left(\frac{\partial u}{\partial z} + \frac{\partial w}{\partial \eta} \right)$$

subject to the dimensionless initial and boundary conditions

$$(3.14) \quad w(\eta, z, 0) = w_0, \quad T(\eta, z, 0) = T_0, \quad C(\eta, z, 0) = C_0$$

$$(3.15) \quad w(\eta, z, t) = u(\eta, z, t) = 0, T(\eta, z, t) = T_w, C(\eta, z, t) = C_w \quad \text{on} \quad \eta = R(z)$$

$$(3.16) \quad \frac{\partial w(\eta, z, t)}{\partial \eta} = \frac{\partial T(\eta, z, t)}{\partial \eta} = \frac{\partial C(\eta, z, t)}{\partial \eta} = u(\eta, z, t) = 0, \quad \text{on} \quad \eta = 0$$

4. SOLUTION OF THE PROBLEM

To obtain the numerical solution, we first of all, transform our cylindrical domain into the rectangular domain by using the following radial transformation. We introduce new variable ξ such that $\xi = \frac{\eta}{R(z)}$. Making use of this transformation, equations (3.4) to (3.16) becomes equations (4.1) to (4.12).

$$(4.1) \quad \frac{1}{R} \frac{\partial u}{\partial \xi} + \frac{u}{R\xi} + \frac{\partial w}{\partial z} - \frac{\xi}{R} \frac{dR}{dz} \frac{\partial w}{\partial \xi} = 0$$

$$(4.2) \quad \frac{\partial u}{\partial t} = -\frac{\partial P}{R\partial \xi} - \frac{u\partial u}{R\partial \xi} - w \left(\frac{\partial u}{\partial z} - \frac{\xi}{R} \frac{dR}{dz} \frac{\partial u}{\partial \xi} \right) + \frac{1}{R} \frac{\partial \tau_{\xi\xi}}{\partial \xi} + \frac{\tau_{\xi\xi}}{R\xi} + \frac{\partial \tau_{\xi z}}{\partial z} - \frac{\xi}{R} \frac{dR}{dz} \frac{\partial \tau_{\xi z}}{\partial \xi}$$

$$\frac{\partial w}{\partial t} = (A_0 + A_1 \cos(\omega t)) - \frac{u\partial w}{R\partial \xi} - w \left(\frac{\partial w}{\partial z} - \frac{\xi}{R} \frac{dR}{dz} \frac{\partial w}{\partial \xi} \right) + \frac{1}{R} \frac{\partial \tau_{\xi z}}{\partial \xi} + \frac{\tau_{\xi z}}{R\xi} + \frac{\partial \tau_{zz}}{\partial z}$$

$$(4.3) \quad -\frac{\xi}{R} \frac{dR}{dz} \frac{\partial \tau_{zz}}{\partial \xi} + a_0 \cos(\omega_b t + \psi) - \frac{H_a^2}{R_e G} w$$

$$\begin{aligned}
(4.4) \quad \frac{\partial T}{\partial t} &= -\frac{u\partial T}{R\partial\xi} - w\left(\frac{\partial T}{\partial z} - \frac{\xi}{R}\frac{dR}{dz}\frac{\partial T}{\partial\xi}\right) + \frac{1}{P_e}\left(\frac{\partial^2 T}{R^2\partial\xi^2} + \frac{1}{R^2\xi}\frac{\partial T}{\partial\xi} + \frac{\partial^2 T}{\partial z^2}\right) \\
&+ \frac{1}{P_e}\left[\frac{3\xi}{R^2}\left(\frac{dR}{dz}\right)^2\frac{\partial T}{\partial\xi} - \frac{2\xi}{R}\frac{dR}{dz}\frac{\partial^2 T}{\partial\xi\partial z} - \frac{\xi}{R}\frac{d^2R}{dz^2}\frac{\partial T}{\partial\xi} + 2\left(\frac{\xi}{R}\frac{dR}{dz}\right)^2\frac{\partial^2 T}{\partial\xi^2}\right] \\
&+ E_c\left(\frac{\tau_{\xi\xi}}{R}\frac{\partial u}{\partial\xi} + \frac{\tau_{\xi z}}{R}\frac{\partial w}{\partial\xi}\right) + E_c\tau_{\xi z}\left(\frac{\partial u}{\partial z} - \frac{\xi}{R}\frac{dR}{dz}\frac{\partial u}{\partial\xi}\right) + E_c\tau_{zz}\left(\frac{\partial w}{\partial z} - \frac{\xi}{R}\frac{dR}{dz}\frac{\partial w}{\partial\xi}\right) \\
(4.5) \quad \frac{\partial C}{\partial t} &= -\frac{u\partial C}{R\partial\xi} - w\left(\frac{\partial C}{\partial z} - \frac{\xi}{R}\frac{dR}{dz}\frac{\partial C}{\partial\xi}\right) + \frac{1}{P_e}\left(\frac{\partial^2 C}{R^2\partial\xi^2} + \frac{1}{R^2\xi}\frac{\partial C}{\partial\xi} + \frac{\partial^2 C}{\partial z^2}\right) \\
&+ \frac{1}{P_e}\left[\frac{3\xi}{R^2}\left(\frac{dR}{dz}\right)^2\frac{\partial C}{\partial\xi} - \frac{2\xi}{R}\frac{dR}{dz}\frac{\partial^2 C}{\partial\xi\partial z} - \frac{\xi}{R}\frac{d^2R}{dz^2}\frac{\partial C}{\partial\xi} + 2\left(\frac{\xi}{R}\frac{dR}{dz}\right)^2\frac{\partial^2 C}{\partial\xi^2}\right] - \frac{\beta C}{Re} \\
&+ S_r\left[\frac{3\xi}{R^2}\left(\frac{dR}{dz}\right)^2\frac{\partial T}{\partial\xi} - \frac{2\xi}{R}\frac{dR}{dz}\frac{\partial^2 T}{\partial\xi\partial z} - \frac{\xi}{R}\frac{d^2R}{dz^2}\frac{\partial T}{\partial\xi} + 2\left(\frac{\xi}{R}\frac{dR}{dz}\right)^2\frac{\partial^2 T}{\partial\xi^2}\right]
\end{aligned}$$

With,

$$(4.6) \quad \dot{\gamma} = \sqrt{2\left[\left(\frac{\partial u}{R\partial\xi}\right)^2 + \left(\frac{u}{R\xi}\right)^2 + \left(\frac{\partial w}{\partial z} - \frac{\xi}{R}\frac{dR}{dz}\frac{\partial w}{\partial\xi}\right)^2\right] + \left(\frac{\partial u}{\partial z} - \frac{\xi}{R}\frac{dR}{dz}\frac{\partial u}{\partial\xi} + \frac{\partial w}{R\partial\xi}\right)^2}$$

and

$$(4.7) \quad \tau_{\xi\xi} = 2(R_{eG}\dot{\gamma}^{n-1} + \tau_0\dot{\gamma}^{-1})\left(\frac{\partial u}{R\partial\xi}\right)$$

$$(4.8) \quad \tau_{zz} = 2(R_{eG}\dot{\gamma}^{n-1} + \tau_0\dot{\gamma}^{-1})\left(\frac{\partial w}{\partial z} - \frac{\xi}{R}\frac{dR}{dz}\frac{\partial w}{\partial\xi}\right)$$

$$(4.9) \quad \tau_{\xi z} = 2(R_{eG}\dot{\gamma}^{n-1} + \tau_0\dot{\gamma}^{-1})\left(\frac{\partial u}{\partial z} - \frac{\xi}{R}\frac{dR}{dz}\frac{\partial u}{\partial\xi} + \frac{\partial w}{\partial\eta}\right)$$

subject to conditions in equations (4.10)to (4.12).

$$(4.10) \quad w(\xi, z, 0) = w_0, \quad T(\xi, z, 0) = T_0, \quad C(\xi, z, 0) = C_0$$

$$(4.11) \quad w(\xi, z, t) = u(\xi, z, t) = 0, \quad T(\xi, z, t) = T_w, C(\xi, z, t) = C_w \quad \text{on} \quad \xi = 1$$

$$(4.12) \quad \frac{\partial w(\xi, z, t)}{\partial\xi} = \frac{\partial T(\xi, z, t)}{\partial\xi} = \frac{\partial C(\xi, z, t)}{\partial\xi} = u(\xi, z, t) = 0, \quad \text{on} \quad \xi = 0$$

We use the initial velocity w_0 , which is obtained as the solution at steady state in the absence of body acceleration and magnetic fields. Applying the radial transformation, the initial velocity is as given in equation (4.13).

$$(4.13) \quad w_0 = \left(\frac{A_0 + A_1}{4}\right)(1 - (H\xi)^2)$$

4.1. The Radial Momentum. We are now going to obtain the radial velocity. We use the continuity equation (4.1) to get the radial velocity $u(\xi, z, t)$. We multiply equation (4.1) by ξR and then integrate it with respect to ξ to obtain equation (4.14).

$$(4.14) \quad \int \xi \frac{\partial u}{\partial \xi} d\xi + \int u d\xi + \int \xi R \frac{\partial w}{\partial z} d\xi + \int \xi^2 \frac{dR}{dz} \frac{\partial w}{\partial \xi} d\xi$$

Re-arranging equation (4.14) we get equation (4.15).

$$(4.15) \quad \int \xi \frac{\partial u}{\partial \xi} d\xi + \int u d\xi = \int \xi^2 \frac{dR}{dz} \frac{\partial w}{\partial \xi} d\xi - \int \xi R \frac{\partial w}{\partial z} d\xi$$

Applying integration by parts and simplifying the equation (4.15) we have equation (4.16).

$$(4.16) \quad u = \frac{dR}{dz} \xi w - \frac{2}{\xi} \frac{dR}{dz} \int w \xi d\xi - \frac{R}{\xi} \int \xi \frac{\partial w}{\partial z} d\xi$$

Making use of the boundary conditions in equations (4.11) and (4.12) and re-arranging we have

$$(4.17) \quad \frac{2}{\xi} \frac{dR}{dz} \int_0^1 w \xi d\xi = -\frac{R}{\xi} \int_0^1 \xi \frac{\partial w}{\partial z} d\xi$$

multiplying by ξ and dividing by R we get (4.18)

$$(4.18) \quad \frac{2}{R} \frac{dR}{dz} \int_0^1 w \xi d\xi = -\int_0^1 \xi \frac{\partial w}{\partial z} d\xi$$

making comparison of the integrals and the integrands of equation (4.18), we easily get equation

$$(4.19) \quad \frac{\partial w}{\partial z} = -\frac{2}{R} \frac{dR}{dz} w$$

We now substitute equation (4.19) into equation (4.16). Such substitution gives equation

$$(4.20) \quad u = \frac{dR}{dz} \xi w - \frac{2}{\xi} \frac{dR}{dz} \int w \xi d\xi - \frac{R}{\xi} \int \xi \left(-\frac{2}{R} \frac{dR}{dz} w \right) d\xi$$

which simplifies to equation (4.21)

$$(4.21) \quad u = \left(\xi \frac{dR}{dz} w \right)$$

Equation (4.21) above, is the radial velocity component which needs to be calculated as well.

However, we substitute this radial velocity into our axial momentum, energy and concentration equations. Also, using the product rule we find the derivatives, $\frac{\partial u}{\partial \xi} = \frac{dR}{dz} \left(\xi \frac{\partial w}{\partial \xi} + w \right)$ and $\frac{\partial u}{\partial z} = \xi \left(\frac{dR}{dz} \frac{\partial w}{\partial z} + w \frac{d^2 R}{dz^2} \right)$. This process therefore eliminates u , as we write radial velocity u in terms of axial velocity w . We now have equations (4.22) to (4.28);

$$(4.22) \quad \frac{\partial w}{\partial t} = (A_0 + A_1 \cos(\omega t)) - \left(\xi \frac{dR}{dz} w \right) \frac{\partial w}{R \partial \xi} - w \left(\frac{\partial w}{\partial z} - \frac{\xi}{R} \frac{dR}{dz} \frac{\partial w}{\partial \xi} \right) + \frac{1}{R} \frac{\partial \tau_{\xi z}}{\partial \xi} + \frac{\tau_{\xi z}}{R \xi} + \frac{\partial \tau_{zz}}{\partial z}$$

$$\begin{aligned} & - \frac{\xi}{R} \frac{dR}{dz} \frac{\partial \tau_{zz}}{\partial \xi} + a_0 \cos(\omega_b t + \psi) - \frac{H_a^2}{Re_G} w \\ \frac{\partial T}{\partial t} = & - \left(\xi \frac{dR}{dz} w \right) \frac{\partial T}{\partial \xi} - w \left(\frac{\partial T}{\partial z} - \frac{\xi}{R} \frac{dR}{dz} \frac{\partial T}{\partial \xi} \right) + \frac{1}{Pe} \left(\frac{\partial^2 T}{R^2 \partial \xi^2} + \frac{1}{R^2 \xi} \frac{\partial T}{\partial \xi} + \frac{\partial^2 T}{\partial z^2} \right) \\ & + \frac{1}{Pe} \left[\frac{3\xi}{R^2} \left(\frac{dR}{dz} \right)^2 \frac{\partial T}{\partial \xi} - \frac{2\xi}{R} \frac{dR}{dz} \frac{\partial^2 T}{\partial \xi \partial z} - \frac{\xi}{R} \frac{d^2 R}{dz^2} \frac{\partial T}{\partial \xi} + 2 \left(\frac{\xi}{R} \frac{dR}{dz} \right)^2 \frac{\partial^2 T}{\partial \xi^2} \right] \end{aligned}$$

$$(4.23) \quad \begin{aligned} & + E_c \left[\frac{\tau_{\xi \xi}}{R} \frac{dR}{dz} \left(\xi \frac{\partial w}{\partial \xi} + w \right) + \frac{\tau_{\xi z}}{R} \frac{\partial w}{\partial \xi} \right] + E_c \tau_{\xi z} \left[\xi \left(\frac{dR}{dz} \frac{\partial w}{\partial z} + w \frac{d^2 R}{dz^2} \right) \right] \\ & - E_c \tau_{\xi z} \left[\frac{\xi}{R} \left(\frac{dR}{dz} \right)^2 \left(\xi \frac{\partial w}{\partial \xi} + w \right) \right] + E_c \tau_{\xi z} \left(\frac{\partial w}{\partial z} - \frac{\xi}{R} \frac{dR}{dz} \frac{\partial w}{\partial \xi} \right) \end{aligned}$$

$$\begin{aligned} \frac{\partial C}{\partial t} = & - \left(\xi \frac{dR}{dz} w \right) \frac{\partial C}{\partial \xi} - w \left(\frac{\partial C}{\partial z} - \frac{\xi}{R} \frac{dR}{dz} \frac{\partial C}{\partial \xi} \right) + \frac{1}{Pe} \left(\frac{\partial^2 C}{R^2 \partial \xi^2} + \frac{1}{R^2 \xi} \frac{\partial C}{\partial \xi} + \frac{\partial^2 C}{\partial z^2} \right) \\ & + \frac{1}{Pe} \left[\frac{3\xi}{R^2} \left(\frac{dR}{dz} \right)^2 \frac{\partial C}{\partial \xi} - \frac{2\xi}{R} \frac{dR}{dz} \frac{\partial^2 C}{\partial \xi \partial z} - \frac{\xi}{R} \frac{d^2 R}{dz^2} \frac{\partial C}{\partial \xi} + 2 \left(\frac{\xi}{R} \frac{dR}{dz} \right)^2 \frac{\partial^2 C}{\partial \xi^2} \right] \\ & + S_r \left[\frac{3\xi}{R^2} \left(\frac{dR}{dz} \right)^2 \frac{\partial T}{\partial \xi} - \frac{2\xi}{R} \frac{dR}{dz} \frac{\partial^2 T}{\partial \xi \partial z} - \frac{\xi}{R} \frac{d^2 R}{dz^2} \frac{\partial T}{\partial \xi} + 2 \left(\frac{\xi}{R} \frac{dR}{dz} \right)^2 \frac{\partial^2 T}{\partial \xi^2} \right] \end{aligned}$$

$$(4.24) \quad + S_r \left(\frac{\partial^2 T}{R^2 \partial \xi^2} + \frac{1}{R^2 \xi} \frac{\partial T}{\partial \xi} + \frac{\partial^2 T}{\partial z^2} \right) - \frac{\beta C}{Re}$$

With,

$$(4.25) \quad \dot{\gamma} = \sqrt{2 \left[\left(\frac{dR}{Rdz} \left(\xi \frac{\partial w}{\partial \xi} + w \right) \right)^2 + \left(\frac{dR}{Rdz} w \right)^2 + \left(\frac{\partial w}{dz} - \frac{\xi}{R} \frac{dR}{dz} \frac{\partial w}{\partial \xi} \right)^2 \right] + \left(\xi \left(\frac{dR}{dz} \frac{\partial w}{\partial z} + w \frac{d^2 R}{dz^2} \right) - \frac{\xi}{R} \frac{dR}{dz} \frac{dR}{dz} \left(\xi \frac{\partial w}{\partial \xi} + w \right) + \frac{\partial w}{R \partial \xi} \right)^2}$$

and

$$(4.26) \quad \tau_{\xi\xi} = 2(R_{eG}\dot{\gamma}^{n-1} + \tau_0\dot{\gamma}^{-1}) \left(\frac{dR}{dz} \left(\xi \frac{\partial w}{\partial \xi} + w \right) \right)$$

$$(4.27) \quad \tau_{zz} = 2(R_{eG}\dot{\gamma}^{n-1} + \tau_0\dot{\gamma}^{-1}) \left(\frac{\partial w}{\partial z} - \frac{\xi}{R} \frac{dR}{dz} \frac{\partial w}{\partial \xi} \right)$$

$$(4.28) \quad \tau_{\xi z} = 2(R_{eG}\dot{\gamma}^{n-1} + \tau_0\dot{\gamma}^{-1}) \left[\xi \left(\frac{dR}{dz} \frac{\partial w}{\partial z} + w \frac{d^2 R}{dz^2} \right) - \frac{\xi}{R} \left(\frac{dR}{dz} \right)^2 \left(\xi \frac{\partial w}{\partial \xi} + w \right) + \frac{\partial w}{R \partial \xi} \right]$$

4.2. Numerical Procedure. In this sub-section, we move from continuous model equations to discrete model equations through discretization. The finite difference schemes for discretization of our model equations are based on the forward difference approximations for time derivatives and central for all spatial derivatives, using the explicit finite difference method. This method was also used by [10] and [11]. The approximate derivatives are as given in equations (4.29) and (4.30).

$$(4.29) \quad \frac{\partial w}{\partial \xi} = \frac{w_{i,j+1}^k - w_{i,j-1}^k}{2\Delta\xi}, \quad \frac{\partial^2 w}{\partial \xi^2} = \frac{w_{i,j+1}^k - 2w_{i,j}^k + w_{i,j-1}^k}{(\Delta\xi)^2}, \quad \frac{\partial w}{\partial t} = \frac{w_{i,j}^{k+1} - w_{i,j}^k}{\Delta t}$$

The approximate derivatives for temperature and concentration are obtained in a similar way as in equation (4.29)

Similarly, the approximations of derivatives of $\tau_{\xi z}$, and τ_{zz} are as given in equation (4.30)

$$(4.30) \quad \frac{\partial \tau_{\xi z}}{\partial \xi} = \frac{(\tau_{\xi z})_{i,j+1}^k - (\tau_{\xi z})_{i,j-1}^k}{2\Delta\xi}, \quad \frac{\partial \tau_{zz}}{\partial \xi} = \frac{(\tau_{zz})_{i,j+1}^k - (\tau_{zz})_{i,j-1}^k}{2\Delta\xi}, \quad \frac{\partial \tau_{zz}}{\partial z} = \frac{(\tau_{zz})_{i+1,j}^k - (\tau_{zz})_{i-1,j}^k}{2\Delta z}$$

We here now define $\xi_j = (j-1)\Delta\xi; j = 1, 2, 3 \dots N+1$ where, $\xi_{N+1} = 1, z_i = (j-1)\Delta z; i = 1, 2, 3 \dots M+1$ and $t_k = (k-1)\Delta t; k = 1, 2, 3 \dots$

We now substitute finite difference schemes into equations (4.22) – (4.28) and we make subject w, T , and C . We also include the discretization of radial velocity from equation

(4.21). We therefore have equations (4.31)-(4.40).

$$(4.31) \quad u_{i,j}^{k+1} = \xi_j \left(\frac{dR}{dz} \right)_i w_{i,j}^k$$

$$(4.32) \quad \begin{aligned} w_{i,j}^{k+1} = & w_{i,j}^k + \Delta t \left(A_0 + A_1 \cos(\omega t_k) + a_0 \cos(\omega_b t_k + \psi) - \frac{H_a^2}{ReG} w_{i,j}^k \right) \\ & - \Delta t \left(\frac{\xi_j}{R_i} \left(\frac{dR}{dz} \right)_i w_{i,j}^k \right) \left(\frac{w_{i,j+1}^k - w_{i,j-1}^k}{2\Delta\xi} \right) - \Delta t w_{i,j}^k \left(\frac{w_{i+1,j}^k - w_{i-1,j}^k}{2\Delta z} \right) \\ & + \Delta t w_{i,j}^k \frac{\xi_j}{R_i} \left(\frac{dR}{dz} \right)_i \left(\frac{w_{i,j+1}^k - w_{i,j-1}^k}{2\Delta\xi} \right) - \frac{\xi_j}{R_i} \left(\frac{dR}{dz} \right)_i \left(\frac{(\tau_{zz})_{i,j+1}^k - (\tau_{zz})_{i,j-1}^k}{2\Delta\xi} \right) \\ & + \Delta t \left[\frac{1}{R_i} \left(\frac{(\tau_{\xi z})_{i,j+1}^k - (\tau_{\xi z})_{i,j-1}^k}{2\Delta\xi} \right) + \frac{(\tau_{\xi z})_{i,j}^k}{R_i \xi_j} + \left(\frac{(\tau_{zz})_{i+1,j}^k - (\tau_{zz})_{i-1,j}^k}{2\Delta z} \right) \right] \end{aligned}$$

$$(4.33) \quad \begin{aligned} T_{i,j}^{k+1} = & T_{i,j}^k - \Delta t \left[\frac{\xi_j}{R_i} \left(\frac{dR}{dz} \right)_i (w_{i,j}^k) \left(\frac{T_{i,j+1}^k - T_{i,j-1}^k}{2\Delta\xi} \right) \right] - \Delta t w_{i,j}^k \left(\frac{T_{i+1,j}^k - T_{i-1,j}^k}{2\Delta z} \right) \\ & + \Delta t \left[w_{i,j}^k \frac{\xi_j}{R_i} \left(\frac{dR}{dz} \right)_i \left(\frac{T_{i,j+1}^k - T_{i,j-1}^k}{2\Delta\xi} \right) \right] + \frac{\Delta t}{P_e} \left(\frac{T_{i,j+1}^k - 2T_{i,j}^k + T_{i,j-1}^k}{R_i^2 (\Delta\xi)^2} \right) \\ & + \frac{\Delta t}{P_e} \left[\frac{T_{i,j+1}^k - T_{i,j-1}^k}{2\xi_j R_i^2 \Delta\xi} + \frac{T_{i+1,j}^k - 2T_{i,j}^k + T_{i-1,j}^k}{(\Delta z)^2} \right] + \frac{\Delta t}{P_e} \left[\frac{3\xi_j}{R_i^2} \left(\frac{dR}{dz} \right)_i^2 \left(\frac{T_{i,j+1}^k - T_{i,j-1}^k}{2\Delta\xi} \right) \right] \\ & - \frac{2\xi_j (\Delta t)}{P_e R_i} \left(\frac{dR}{dz} \right)_i \left(\frac{T_{i+1,j+1}^k - T_{i-1,j+1}^k - T_{i+1,j-1}^k + T_{i-1,j-1}^k}{4\Delta\xi \Delta z} \right) \\ & - \frac{\Delta t}{P_e} \left[\frac{\xi_j}{R_i} \left(\frac{d^2 R}{dz^2} \right)_i \left(\frac{T_{i,j+1}^k - T_{i,j-1}^k}{2\Delta\xi} \right) \right] + \frac{2\Delta t}{P_e} \left(\frac{\xi_j}{R_i} \frac{dR}{dz} \right)_i^2 \left(\frac{T_{i,j+1}^k - 2T_{i,j}^k + T_{i,j-1}^k}{(\Delta\xi)^2} \right) \\ & + \Delta t E_c \left[\frac{(\tau_{\xi\xi})_{i,j}^k}{R_i} \left(\frac{dR}{dz} \right)_i \left(\xi_j \left(\frac{w_{i,j+1}^k - w_{i,j-1}^k}{2\Delta\xi} \right) + w_{i,j}^k \right) + \frac{(\tau_{\xi z})_{i,j}^k}{R_i} \left(\frac{w_{i,j+1}^k - w_{i,j-1}^k}{2\Delta\xi} \right) \right] \\ & + \Delta t E_c (\tau_{\xi z})_{i,j}^k \left[\xi_j \left(\left(\frac{dR}{dz} \right)_i \left(\frac{w_{i+1,j}^k - w_{i-1,j}^k}{2\Delta z} \right) + w_{i,j}^k \left(\frac{d^2 R}{dz^2} \right)_i \right) \right] \\ & - \Delta t E_c (\tau_{\xi z})_{i,j}^k \left[\frac{\xi_j}{R_i} \left(\frac{dR}{dz} \right)_i^2 \left(\xi_j \left(\frac{w_{i,j+1}^k - w_{i,j-1}^k}{2\Delta\xi} \right) + w_{i,j}^k \right) \right] + \Delta t E_c (\tau_{\xi z})_{i,j}^k \left(\frac{w_{i+1,j}^k - w_{i-1,j}^k}{2\Delta z} \right) \\ & - \Delta t E_c (\tau_{\xi z})_{i,j}^k \frac{\xi_j}{R_i} \left(\frac{dR}{dz} \right)_i \left(\frac{w_{i,j+1}^k - w_{i,j-1}^k}{2\Delta\xi} \right) \end{aligned}$$

$$\begin{aligned}
C_{i,j}^{k+1} = & C_{i,j}^k - \Delta t \left[\frac{\xi_j}{R_i} \left(\frac{dR}{dz} \right)_i \left(w_{i,j}^k \right) \left(\frac{C_{i,j+1}^k - C_{i,j-1}^k}{2\Delta\xi} \right) \right] \\
& - \Delta t \left[w_{i,j}^k \left(\frac{C_{i+1,j}^k - C_{i-1,j}^k}{2\Delta z} - \frac{\xi_j}{R_i} \left(\frac{dR}{dz} \right)_i \left(\frac{C_{i,j+1}^k - C_{i,j-1}^k}{2\Delta\xi} \right) \right) \right] \\
& + \frac{\Delta t}{P_e} \left[\frac{C_{i,j+1}^k - 2C_{i,j}^k + C_{i,j-1}^k}{R_i^2 (\Delta\xi)^2} + \frac{C_{i,j+1}^k - C_{i,j-1}^k}{2\xi_j R_i^2 \Delta\xi} + \frac{C_{i+1,j}^k - 2C_{i,j}^k + C_{i-1,j}^k}{(\Delta z)^2} \right]
\end{aligned}$$

(4.34)

$$\begin{aligned}
& + \frac{\Delta t}{S_c R_e} \left[\frac{3\xi_j}{R_i^2} \left(\frac{dR}{dz} \right)_i^2 \left(\frac{C_{i,j+1}^k - C_{i,j-1}^k}{2\Delta\xi} \right) \right] \\
& - \frac{2\xi_j (\Delta t)}{P_e R_i} \left(\frac{dR}{dz} \right)_i \left(\frac{C_{i+1,j+1}^k - C_{i-1,j+1}^k - C_{i+1,j-1}^k + C_{i-1,j-1}^k}{4\Delta\xi \Delta z} \right) \\
& - \frac{\Delta t}{P_e} \left[\frac{\xi_j}{R_i} \left(\frac{d^2 R}{dz^2} \right)_i \left(\frac{C_{i,j+1}^k - C_{i,j-1}^k}{2\Delta\xi} \right) \right] + \frac{2\Delta t}{P_e} \left(\frac{\xi_j}{R_i} \frac{dR}{dz} \right)_i^2 \left(\frac{C_{i,j+1}^k - 2C_{i,j}^k + C_{i,j-1}^k}{(\Delta\xi)^2} \right) \\
& + S_r \Delta t \frac{3\xi_j}{R_i^2} \left(\frac{dR}{dz} \right)_i^2 \left(\frac{T_{i,j+1}^k - T_{i,j-1}^k}{2\Delta\xi} \right) - \frac{2\xi_j \Delta t}{R_i} \left(\frac{dR}{dz} \right)_i \left(\frac{T_{i+1,j+1}^k - T_{i-1,j+1}^k - T_{i+1,j-1}^k + T_{i-1,j-1}^k}{4\Delta\xi \Delta z} \right) \\
& - S_r \Delta t \left[\frac{\xi_j}{R_i} \left(\frac{d^2 R}{dz^2} \right)_i \left(\frac{T_{i,j+1}^k - T_{i,j-1}^k}{2\Delta\xi} \right) \right] + 2\Delta t S_r \left(\frac{\xi_j}{R_i} \right)^2 \left(\frac{dR}{dz} \right)_i^2 \left(\frac{T_{i,j+1}^k - 2T_{i,j}^k + T_{i,j-1}^k}{(\Delta\xi)^2} \right)
\end{aligned}$$

With,

$$(4.35) \quad \gamma^2 = 2 \left[\left(\left(\frac{dR}{dz} \right)_i \left(\xi_j \left(\frac{w_{i,j+1}^k - w_{i,j-1}^k}{2\Delta\xi} + w_{i,j}^k \right) \right) \right)^2 + \left(\left(\frac{1}{R_i} \right) \left(\frac{dR}{dz} \right)_i w_{i,j}^k \right)^2 \right]$$

$$(4.36) \quad + 2 \left(\frac{w_{i+1,j}^k - w_{i-1,j}^k}{2\Delta z} - \frac{\xi_j}{R_i} \left(\frac{dR}{dz} \right)_i \left(\frac{w_{i,j+1}^k - w_{i,j-1}^k}{2\Delta\xi} \right) \right)^2$$

$$(4.37) \quad + \left\{ \left[\xi_j \left(\frac{dR}{dz} \right)_i \left(\frac{w_{i+1,j}^k - w_{i-1,j}^k}{2\Delta z} \right) + w_{i,j}^k \left(\frac{d^2 R}{dz^2} \right)_i \right] \right. \\ \left. - \left[\frac{\xi_j}{R_i} \left(\frac{dR}{dz} \right)_i^2 \left(\xi_j \frac{w_{i,j+1}^k - w_{i,j-1}^k}{2\Delta\xi} + w_{i,j}^k \right) + \frac{1}{R_i} \frac{w_{i,j+1}^k - w_{i,j-1}^k}{2\Delta\xi} \right] \right\}$$

and

$$(4.38) \quad (\tau_{\xi\xi})_{i,j}^k = 2 (R_{eG} \gamma^{n-1} + \tau_0 \dot{\gamma}^{-1}) \left(\left(\frac{dR}{dz} \right)_i \left(\xi_j \frac{w_{i,j+1}^k - w_{i,j-1}^k}{2\Delta\xi} + w_{i,j}^k \right) \right)$$

(4.39)

$$(\tau_{\xi z})_{i,j}^k = 2(R_{eG}\dot{\gamma}^{n-1} + \tau_0\dot{\gamma}^{-1}) \left[\begin{array}{l} \xi_j \left(\left(\frac{dR}{dz} \right)_i \left(\frac{w_{i+1,j}^k - w_{i-1,j}^k}{2\Delta z} \right) \right) + w_{i,j}^k \left(\frac{d^2R}{dz^2} \right)_i - \\ \frac{\xi_j}{R_i} \left(\frac{dR}{dz} \right)_i^2 \left(\xi_j \frac{w_{i,j+1}^k - w_{i,j-1}^k}{2\Delta \xi} + w_{i,j}^k \right) + \frac{w_{i,j+1}^k - w_{i,j-1}^k}{2R_i\Delta \xi} \end{array} \right]$$

(4.40)

$$(\tau_{zz})_{i,j}^k = 2(R_{eG}\dot{\gamma}^{n-1} + \tau_0\dot{\gamma}^{-1}) \left[\frac{w_{i+1,j}^k - w_{i-1,j}^k}{2\Delta z} - \frac{\xi_j}{R_i} \left(\frac{dR}{dz} \right)_i \left(\frac{w_{i,j+1}^k - w_{i,j-1}^k}{2\Delta \xi} \right) \right]$$

The conditions in equations (4.10) to (4.12) are discretized as shown in equations (4.41) and

(4.42)

$$(4.41) \quad w_{i,j}^1 = w_0, \quad T_{i,j}^1 = T_0, \quad C_{i,j}^1 = C_0; \quad w_{i,2}^k = w_{i,1}^k, \quad T_{i,2}^k = T_{i,1}^k, \quad C_{i,2}^k = C_{i,1}^k$$

$$(4.42) \quad w_{i,N+1}^k = 0, \quad u_{i,N+1}^k = 0, \quad T_{i,N+1}^k = T_w, \quad C_{i,N+1}^k = C_w, \quad (\tau_{\xi z})_{i,1}^k = 0.$$

5. SIMULATION AND DISCUSSION

In this section, we display and discuss the numerical simulation of the discretized equations (4.31) to (4.40). The simulation was done using MATLAB software using the following parameter values. $A_1 = 0.8$, $A_0 = 0.5$, $\omega_p = 10$, $\omega_b = 10$, $a_0 = 1$, $Ha = 1$, $\psi = 0.3$, $R_{eG} = 1$, $e = 0.1$, $z_0 = 1$, $\Delta t = 0.0002$, $\Delta z = 0.08$, $\Delta \xi = 0.05$, $\tau_0 = 0.2$, $E_c = 1$, $P_e = 1$, $\beta = 0.1$, $S_r = 0.002$ and $n = 0.95$. The parameters were varied to determine their effect.

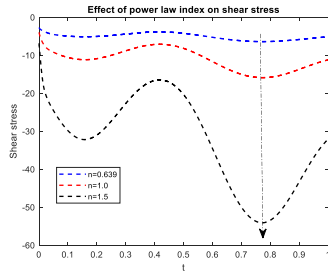


FIGURE 2

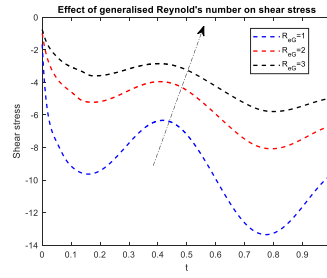


FIGURE 3

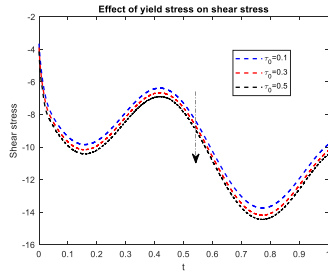


FIGURE 4

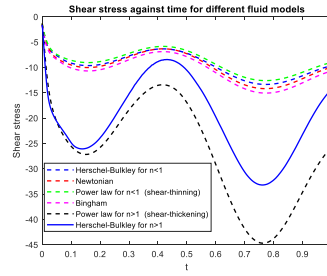


FIGURE 5

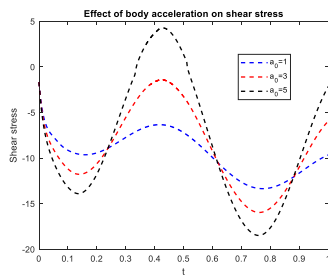


FIGURE 6

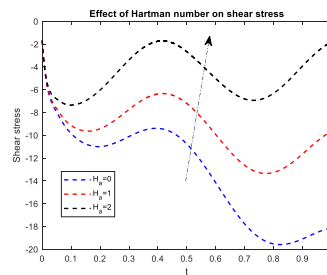


FIGURE 7

Figures 2-7 give the results for shear stresses. From the graphs, it is seen that, the magnitude of shear stress increases as the power law index increases. This is shown in figure 2. Opposite behavior is shown in figure 3, where the magnitude of shear stress declines towards positive values as generalized Reynold's number increases. This implies that as the inertial forces increases, the magnitude of shear stress decreases. Figure 4 illustrates the effect of yield stress on shear stress. It is observed that as the yield stress increases, the shear stress increases in magnitude. This therefore implies that increasing certain the amount of stress required for blood to flow, increases the shear stress. Comparison of shear stress for different fluid behaviors for Herschel-Bulkley, Newtonian, power law and Bingham is illustrated in figure 5. From figure 5 we observe that the power law fluid when $n > 1$ has higher magnitude of shear stress compared to power law fluid for $n < 1$. The same has been observed for Herschel-Bulkley fluid where the higher the power law index the higher the magnitude of shear stress. It is interesting to note further that when power law index $n > 1$ the shear stress exhibits more difference than when $n < 1$ where the difference is small. This tells us that, it deviates more when $n > 1$ than when $n < 1$. Figure 6 shows the effect of body acceleration on shear stress. It is seen that as body acceleration increases, the shear stress increases in magnitude. The opposite trend is observed in figure 7 where, the increase in Hartman number diminishes the magnitude of the shear stress. Hartman number is a ratio of electromagnetic forces to viscous forces. Increasing the Hartman number implies that the viscous forces become lower than the electromagnetic forces. Physically, the Hartman number enhances the Lorentz force which opposes the blood's motion.

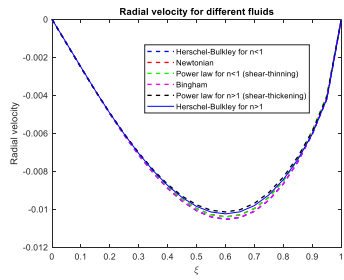


FIGURE 8

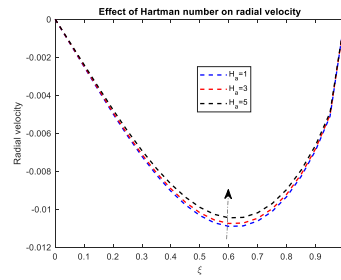


FIGURE 9

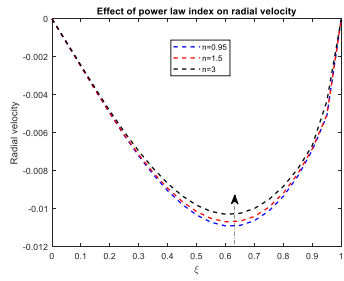


FIGURE 10

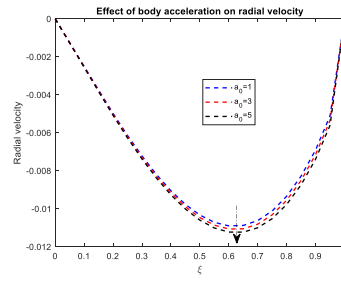


FIGURE 11

The results of radial velocity are presented in figures 8-11. From these figures, it is noted that the radial velocities are negative in sign. The radial velocity is shown to be zero on the axis of symmetry as it was assumed that no radial flow takes place along the axis of the symmetry. The velocity is also zero on the arterial wall ($\xi = 1$) to satisfy the no slip condition. In figure 8 we observe that when the power law index n is greater than 1, the radial velocity exhibits smaller magnitude values than when $n < 1$. From the same figure 8, we observe that radial velocity for Herschel-Bulkley fluid when $n < 1$ has higher values in magnitude as compared to power law, Bingham, Newtonian and Herschel-Bulkley for $n > 1$. It is also observed that radial velocity diminishes in magnitude as Hartman number and power law index increase as shown in figures 9 and 10 respectively. This finding is in good agreement with [10]. On the other hand, it is further shown that increase in body acceleration increases the magnitude of radial velocity. Like in radial velocity, it is also illustrated in axial velocity that body acceleration enhances axial velocity while the Hartman number diminishes the axial velocity due to the Lorentz force which tend to oppose fluid's motion. Furthermore, the axial velocity is shown to increase with increase in steady state part of pressure gradient and the amplitude of pressure oscillation responsible for enhancing the systolic and diastolic pressures. This is as illustrated in figures 12-15 below.

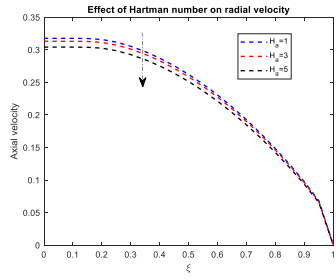


FIGURE 12

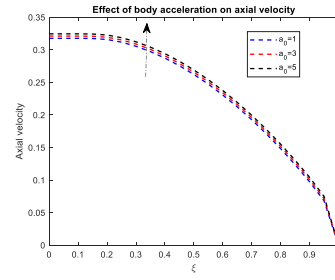


FIGURE 13

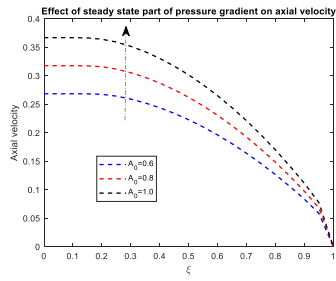


FIGURE 14

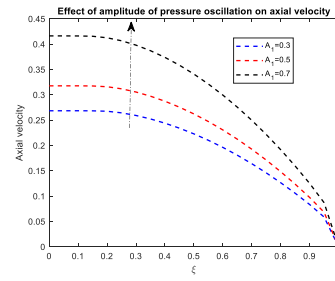


FIGURE 15

Temperature profiles against radial distance are displayed in figures 16-19 below. Figure 16 shows the effect of Peclet number on temperature profile. Peclet number is the ratio of the heat transferred by convection to the heat transferred by conduction. It is observed that, increase in Peclet number diminishes temperature profile. This means that heat transfer by motion of blood increases than heat transfer by conduction. In figure 17 we observe as expected that, increase in body acceleration raises temperature profile. This implies that body exercise give rise to the core body temperature. Eckert number is defined as the ratio of the advective mass transfer to the heat dissipation potential. It offers a measure of the kinetic energy of the flow relative to the enthalpy difference across the thermal boundary layer. It is observed in figure 18 that the increase in Eckert number increases the temperature profile, physically implying that as Eckert number increases, the advective mass transfer dominates the heat dissipation potential and therefore the temperature increases. Figure 19 reveals that as the Hartman number increases, the temperature profile decreases.

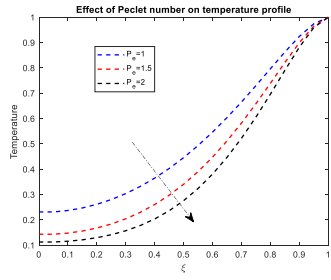


FIGURE 16

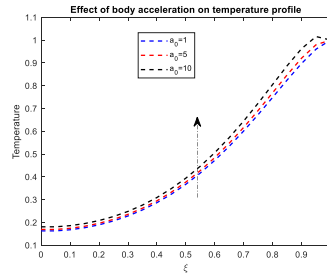


FIGURE 17

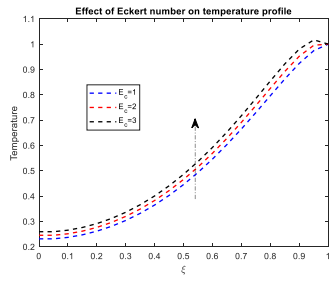


FIGURE 18

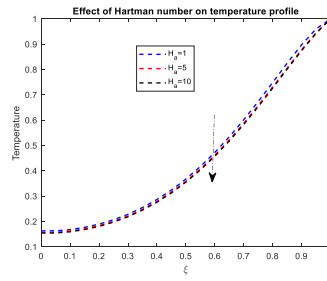


FIGURE 19

The effect of chemical reaction on concentration is observed in figure 20. From the figure, we observe that, the concentration profile decreases with increasing chemical reaction parameter, which implies that the chemical reaction parameter acts as a destructive agent. On the other hand, figure 21 shows the effect of increasing the Soret number on concentration profile. Soret number is the ratio of temperature difference to the concentration. As expected, the concentration profile increases with increasing the Soret number.

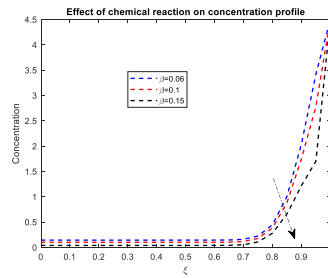


FIGURE 20

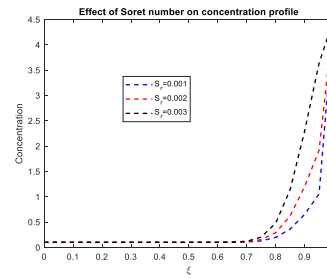


FIGURE 21

6. CONCLUSION

The current study presents numerical results of an unsteady heat and mass transfer blood flow through a stenosed artery in the presence of magnetic field, body acceleration and chemical reaction. Blood is considered to be non-Newtonian of Herschel-Bulkley type. It is established that the presence of magnetic field diminishes the blood's velocity; the body acceleration and Eckert numbers enhance temperature profile; while the concentration profile is reduced by increased chemical reaction. The study strongly suggests that for people with stenosed arteries, physical exercises in hot environment should be done with care. Further, the study has found out that the Herschel-Bulkley fluid experience higher velocity than the power law (for both when $n < 1$ and when $n > 1$), Bingham and Newtonian fluids. For non-Newtonian models, Herschel-Bulkley when $n < 1$ is also observed to be suitable to blood flow than the Bingham and the power law. Further more, shear stress is observed to deviate more when $n > 1$ than when $n < 1$. Considering the difference in shear stress and velocity profiles between the Newtonian and Herschel-Bulkley fluids, it is suggested that it is better to model blood flow using Herschel-Bulkley constitutive model than Newtonian.

CONFLICT OF INTERESTS

The author(s) declare that there is no conflict of interests.

REFERENCES

- [1] M. Y. Abdollahzadeh Jamalabadi, M. Daqiqshirazi, H. Nasiri, M. R. Safaei, and T. K. Nguyen, Modeling and analysis of biomagnetic blood carreau fluid flow through a stenosis artery with magnetic heat transfer: A transient study, *PLoS One*, 13 (2018), e0192138.
- [2] N. S. Akbar, S. Nadeem, and M. Ali, Influence of heat and chemical reactions on hyperbolic tangent fluid model for blood flow through a tapered artery with a stenosis, *Heat Transfer Res.* 43 (2012), 69-94.
- [3] R. D. Alsemiry, P. K. Mandal, H. M. Sayed, N. Amin, et al., Numerical solution of blood flow and mass transport in an elastic tube with multiple stenoses, *BioMed Res. Int.* 2020 (2020), 7609562.
- [4] D. Biswas and R. B. Laskar, Steady flow of blood through a stenosed artery: A non-newtonian fluid model, *Assam Univ. J. Sci. Technol.* 7 (2011), 144–153.
- [5] K. Bunonyo, C. Israel-Cookey, and E. Amos, Mhd oscillatory flow of jeffrey fluid in an indented artery with heat source, *Asian Res. J. Math.* 7 (2017), Article no. ARJOM.37604.
- [6] S. Changdar and S. De, Numerical simulation of nonlinear pulsatile newtonian blood flow through a multiple stenosed artery, *Int. Sch. Res. Not.* 2015 (2015), 628605.
- [7] A. Dixit, A. Gupta, and N. Garg, Observations of blood flow in an inclined improved generalized multiple stenosed artery influenced by a magnetic field, Available at SSRN: <https://dx.doi.org/10.2139/ssrn.3154042>. (2018).
- [8] I. Eldesoky, Unsteady MHD Pulsatile Blood Flow through Porous Medium in a Stenotic Channel with Slip at the Permeable Walls Subjected to Time Dependent Velocity (Injection/Suction), *The International Conference on Mathematics and Engineering Physics.* 7 (2014) 1–25.
- [9] F. J. H. Gijssen, E. Allanic, F. N. van de Vosse, J. D. Janssen, The influence of the non-Newtonian properties of blood on the flow in large arteries: unsteady flow in a 90° curved tube, *J. Biomech.* 32 (1999), 705–713.

- [10] M. A. Iqbal, S. Chakravarty, K. K. Wong, J. Mazumdar, and P. K. Mandal, Unsteady response of non-newtonian blood flow through a stenosed artery in magnetic field, *J. Comput. Appl. Math.* 230 (2009), 243–259.
- [11] Z. Ismail, I. Abdullah, N. Mustapha, and N. Amin, A power-law model of blood flow through a tapered overlapping stenosed artery, *Appl. Math. Comput.* 195 (2008), 669–680.
- [12] D. F. Jamil, R. Roslan, M. Abdulhameed, N. Che-Him, S. Sufahani, M. Mohamad, and M. G. Kamardan, Unsteady blood flow with nanoparticles through stenosed arteries in the presence of periodic body acceleration, *J. Phys.* 995 (2018), 012032.
- [13] S. Kumar, N. Garg, and A. Gupta, Herschel bulkley model for blood flow through an arterial segment with stenosis, *Int. J. Sci. Tech. Manage.* 4 (2015), 93–100.
- [14] Y. Liu and W. Liu, Blood flow analysis in tapered stenosed arteries with the influence of heat and mass transfer, *J. Appl. Math. Comput.* 63 (2020), 523–541.
- [15] J. Misra, S. Adhikary, B. Mallick, and A. Sinha, Mathematical modeling of blood flow in arteries subject to a vibrating environment, *J. Mech. Med. Biol.* 18 (2018), 1850001.
- [16] K. Prasad Maruthi and Y. P. Reddy, Mathematical modelling on an electrically conducting fluid flow in an inclined permeable tube with multiple stenoses, *Int. J. Innov. Technol. Explor. Eng.* 9 (2019), 2278–3075.
- [17] C. Rodkiewicz, P. Sinha, and J. Kennedy, On the application of a constitutive equation for whole human blood., *J. Biomech. Eng.* 112 (1990), 198–206.
- [18] B. D. Sharma and P. K. Yadav, A mathematical model of blood flow in narrow blood vessels in presence of magnetic field, *Nat. Acad. Sci. Lett.* 42 (2019), 239–243.
- [19] A. Sinha, J. Misra, and G. Shit, Effect of heat transfer on unsteady mhd flow of blood in a permeable vessel in the presence of non-uniform heat source, *Alex. Eng. J.* 55 (2016), 2023–2033.
- [20] N. Srivastava, Herschel-bulkley magnetized blood flow model for an inclined tapered artery for an accelerated body, *J. Sci. Technol.* 10 (2018), 53–59.
- [21] C. Tu and M. Deville, Pulsatile flow of non-newtonian fluids through arterial stenoses, *J. Biomech.* 29 (1996), 899–908.

- [22] K. Vajravelu, S. Sreenadh, P. Devaki, and K. Prasad, Mathematical model for a herschel-bulkley fluid flow in an elastic tube, *Open Phys.* 9 (2011), 1357–1365.
- [23] A. Zaman, N. Ali, M. Sajid, and T. Hayat, Effects of unsteadiness and non-newtonian rheology on blood flow through a tapered time-variant stenotic artery, *AIP adv.* 5 (2015), 037129.